



Removal of toxic dye (Rhodamine B) from aqueous solutions by natural smectite (SMC) and SMC-nanoTiO₂

Muna Abd Ul Rasool Al-Kazragi, Dhafir T.A. Al-Heetimi*

Department of Chemistry, College of Education for Pure Science Ibn-Al-Haitham, University of Baghdad, Baghdad, Iraq, Tel. +964-7708826565; emails: dhafir1973@gmail.com/dhafir.t.a@ihcoedu.uobaghdad.edu.iq (D.T.A. Al-Heetimi), muna.ar.k@ihcoedu.uobaghdad.edu.iq/muna.alkazragi@gmail.com (M.A. Al-Kazragi)

Received 2 May 2020; Accepted 2 May 2021

ABSTRACT

Titanium oxide nanoparticles-modified smectite (SMC-nTiO₂) as a low-cost adsorbent was investigated for the removal of Rhodamine B (RhB) from aqueous solutions. The adsorbents (SMC and SMC-nTiO₂) were characterized by scanning electron microscopy, Fourier transforms infrared spectroscopy, and energy-dispersive X-ray spectroscopy. The effects of various parameters like contact time, adsorbent weight, pH, and temperatures were examined. Three kinetic equations (pseudo-first-order (PFO), pseudo-second-order (PSO), and intra-particle diffusion) were used to evaluate the experimental kinetic of the data and the results showed that the adsorption process is in line with the PSO kinetic model. Adsorption equilibrium isotherms were modeled using Langmuir, Freundlich, and Temkin equations. The removal processes of RhB onto SMC and SMC-nTiO₂ were fitted well by the Freundlich isotherm. The maximum cationic dye removal of 91.4% and 99.9% were obtained at pH 9.04, for the adsorbent surfaces SMC and SMC-nTiO₂, respectively. Thermodynamic parameters such as ΔG° , ΔH° , ΔS° , and E_a were also estimated for the whole process. The error function, the nonlinear Chi-square test (χ^2) have been also determined. Titanium oxide nanoparticles- modified smectite clay sample shows very good potential as a low-cost adsorbent for the removal of RhB from aqueous solutions.

Keywords: Nano-TiO₂; Rhodamine B; Smectite; Removal; Freundlich isotherm; Kinetic

1. Introduction

The synthetic dye (Rhodamine B), which is one of the basic xanthene dyes is widely employed in the industries of photographic, food stuffs, printing, textile, and as a water tracer fluorescent material [1]. It has been medically proven that contamination of drinking water with cationic dyes is highly carcinogenic and leads to irritation of the skin, eyes, and respiratory tract [2]. Several well-known treatment technologies can be used to minimize the major problem associated with the pollution caused by this dye. These include physical and chemical processes such as filtration [3], ozonation [4], precipitation [5], photodegradation [6],

coagulation [7], etc. Adsorption technology is one of the attractive treatment methods to remove the dyestuff, pigments, phenolic compounds, and other chemicals from the wastewater due to its high efficiency, ability to treat different kinds of dyes in concentrated form, low-cost, and simplicity of design [8]. Many adsorbents have been used to remove dyes from wastewater. Among them, are bentonite [9], peanut husk [10], polydopamine microspheres [11], and tin oxide nanoparticles [12]. Several research studies have been carried out to investigate the importance and applications of dye treatment via adsorption on natural and synthesized adsorbents. Gupta et al. [13] studied the removal of rhodamine B by bagasse fly ash, solid waste of the

* Corresponding author.

sugar industry, by converting it into an inexpensive adsorbent material. The adsorption data have been correlated with both Langmuir and Freundlich's adsorption models. Thermodynamic parameters have been studied and indicated the feasibility of the process.

Khan et al. evaluated the adsorption efficiency of Rhodamine B (RhB) removal from an aqueous solution by kaolinite as an adsorbent. The Fourier transforms infrared (FTIR) spectra and scanning electron micrographs of the adsorbent, before and after adsorption, indicated dye binding on the kaolinite surface. The optimized conditions for adsorption were studied such as initial concentration of dye, pH, contact time, adsorbent dose, and temperature. The obtained data followed Langmuir isotherm model with monolayer adsorption capacity (q_m) equal to 46.08 mg/g (83%). The kinetic data agreed well with the pseudo-second-order (PSO) model. Adsorption of Rhodamine B dye onto kaolinite was spontaneous, endothermic, and accompanied by an increase in entropy. The study revealed that kaolinite can be used as an efficient low-cost adsorbent for the removal of RhB dye [14]. Yu et al. [15] successfully grafted Graphene oxide (GO) nanosheets and a carboxylated diazonium salt to Zeolite particles surface for the adsorption of rhodamine B from aqueous solutions. The adsorption isotherm was fitted to Langmuir isotherm and shown to follow a PSO reaction model. Neto et al. [16] investigated the removal of Rhodamine B from aqueous solutions using natural and purified bentonite clay. The adsorbents were characterized by X-ray diffraction (XRD), thermogravimetric analysis (TG), its derivative (DTG), and differential thermal analysis (DTA). The Freundlich isotherm produced the best fit for the adsorption data. The experimental data were the best fit by the PSO. The purified clays efficiently removed the rhodamine B [16].

Iraqi smectite (SMC), (as a representative) clay mineral, is composed of the octahedral sheet placed between two side tetrahedral sheets Fig. 1 [17]. Smectite possesses negative charges on the layer sheets, caused by the isomorphous substitution of Mg^{2+} with Al^{3+} in the octahedral layer and Al^{3+} with Si^{4+} in the tetrahedral layer, which is balanced by the presence of exchangeable cations like (Na^+ , Ca^{2+} , or Mg^{2+}). These cations have strong hydration capabilities in

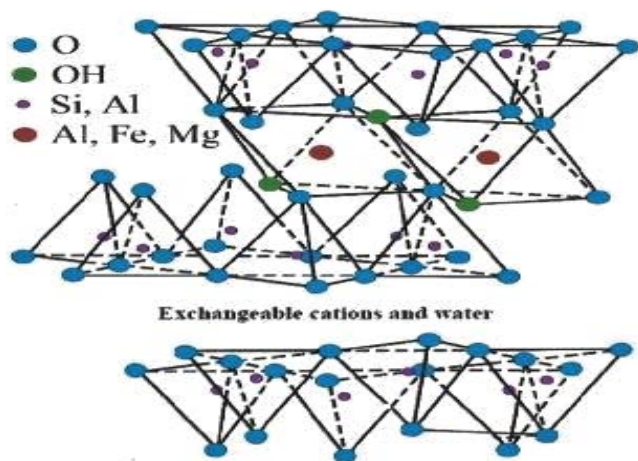


Fig. 1. Structure of smectite clay [17].

the presence of water and facilitate the expansion of smectite after wetting [18]. Nano-scale materials have shown many advantages, such as high surface area, effectiveness, high adsorption capacity [19], and the high number of surface reactive atoms in porous matrices. Commonly the nanoparticles would easily aggregate (due to their magnetic property) [12]. In this study, the removal efficiency of TiO_2 nanoparticles modified smectite (as a new adsorbent) towards basic dye RhB has been investigated and characterized. The optimization of all adsorption experiments and conditions such as contact time, pH, adsorbent dosage, and temperatures were optimized. Moreover, mechanisms with kinetic, thermodynamic models, and RhB adsorption isotherm were measured and discussed.

2. Experimental

2.1. Materials and chemicals

The cationic dye (RhB) $C_{28}H_{31}ClN_2O_3$ was used without any further purification and molecular structure given in Fig. 2. Nano- TiO_2 (M_{wt} 79.86 g/mol, 60 nm, purity > 99.8%) was purchased from Micxy company. Smectite clay (SMC) was supplied from the general company for Geological Survey and Mining, Baghdad, Iraq. The major components of SMC were (K_2O 0.6%, Na_2O 1.1%, MgO 3.4%, CaO 6.0%, Fe_2O_3 5.1%, Al_2O_3 15.7%, SiO_2 56.7%, and L.O.I 9.5%).

2.2. Preparation of SMC and SMC- $nTiO_2$

SMC was firstly washed several times using deionized water to remove impurities and dried in an oven at a temperature of (90°C) for 5 h, cooled at room temperature, then SMC was crushed and sieved to the desired particle size ($\leq 75 \mu m$) and after that kept in airtight container to use in the chemical experiment. 4.0 g nano- TiO_2 was dissolved in 100 mL deionized water, SMC powder (10.0 g) was added into the solution and was sonicated by using Ultrasonic Cleaner Sonicator (Power Sonic 040S) for 30 min at 30°C. Then, the suspension was filtered out, washed with deionized water and dried for 5 h at 90°C. Finally, the modified SMC grounded, sieved to particle size ($\leq 75 \mu m$) and stored in tightly closed bottles to be used for adsorption [20].

2.3. Characterization of SMC and nano- TiO_2 modified SMC (SMC- $nTiO_2$)

SMC and SMC- $nTiO_2$ surface functional groups were detected using the FTIR spectroscopy (Shimadzu 8400,

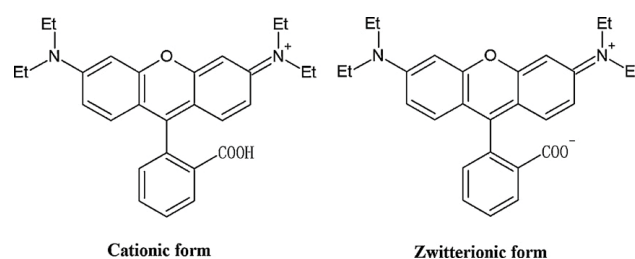


Fig. 2. Molecular form of RhB (cationic and zwitterionic forms).

Japan) in the scanning range of 4,000–400 cm^{-1} . The SMC and SMC-nTiO₂ surface morphology were examined by scanning electron microscopy (SEM) T-SCAN Mira3 France. Energy-dispersive X-ray spectroscopy (EDS, Hitachi, Ltd., Tokyo, Japan) was then performed. Surface area and pore parameters were recorded with a Brunauer–Emmett–Teller surface area analyzer (TriStar II Plus 2.03).

2.4. Determination of zero-point charge of the SMC and SMC-nTiO₂ adsorbents

20 mL of 0.01 M NaCl solution were put into different 100 mL Erlenmeyer flasks with the initial pHs adjusted between 4.37 and 9.63 by adding a few drops of 0.1 M HCl and NaOH in each flask. Then 0.2 and 0.1 g SMC and SMC-nTiO₂ were added to each flask, respectively, and the suspensions were left for 24 h at 25°C. They were centrifuged, and the final pHs of the solutions were determined. The point of intersection of the curves in the plot of ΔpH vs. pH initial gave the pH_{pzc} of the two adsorbents [5].

2.5. Adsorption procedures of SMC and SMC-nTiO₂

A stock solution of RhB of 1,000 mg/L concentration was prepared by dissolving an appropriate amount of dye powder in deionized water. For adsorption isotherms, 0.2 and 0.1 g of SMC and SMC-nTiO₂ were added respectively and separately to 10 mL of RhB solutions of different initial concentrations ranging from 10 to 70 mg/L taken in 100 mL conical flasks. The temperatures of 25°C, 35°C, and 45°C were controlled using an isothermal shaker. After each adsorption process, the samples were centrifuged (Hettich EBA-20, Germany, 6,000 rpm) at 3,000 rpm for 10 min. The clear supernatants were analyzed by a UV-VIS spectrophotometer double beam type T-80 England at 543 nm wavelength.

The RhB removal percentage ($R\%$) and amount of RhB adsorbed q_e were calculated via Eqs. (1) and (2):

$$R\% = \frac{C_0 - C_e}{C_0} \times 100 \quad (1)$$

$$q_e = \frac{(C_0 - C_e)W_t}{V} \quad (2)$$

where C_0 and C_e (mg/L) are the initial RhB and equilibrium RhB concentrations, respectively. While q_e is the amount of RhB dye adsorbed after equilibrium in (mg/g). V (L) is the volume of solution and W_t (g/L) is the weight of the adsorbent.

3. Results and discussion

3.1. FTIR analysis results of SMC and SMC-nTiO₂

The FTIR measurements of SMC and SMC-nTiO₂ surfaces are shown in (Figs. 3a and b). A characteristic band at 3,618 cm^{-1} is attributed to the stretching vibrations of the hydroxyl group. The broadband that appears at 1,631 cm^{-1} may be explained by the bending vibration of the OH group [1].

The absorption bands at 1,035 and 470 cm^{-1} are assigned to the stretching vibration of Si–O–Si group. The band at 918 cm^{-1} represents the bending vibrations of Al–OH [21]. After modification of SMC with nano-TiO₂ (Fig. 3b), the bands around 3,436 and 3,419 cm^{-1} were ascribed to the Ti–OH on the surface of nano-TiO₂. The band at 628 cm^{-1} indicates the stretching vibration of the Ti–O bond of a TiO₂ [22,23]. The weak band at 2,362 cm^{-1} corresponds to the stretching vibration of TiOO–H [24].

3.2. SEM characterization

The SEM images of SMC and SMC-nTiO₂ are illustrated in Figs. 4a and b. The image (Fig. 4a) reveals the drusy texture with high porosity, enveloped crystalline tubular habits. The surface morphology of smectite clay can be supported by different reports available in literature that alumina silicates sheets consist of silica SiO₄ tetrahedra bonded to alumina octahedra in a variety of ways, which have a sheet-like layered structure. A 2:1 ratio of the tetrahedra to the octahedral [25,26]. On the other hand, when the SMC surface was modified with nano-TiO₂ (Fig. 4b), spherical TiO₂ nanoparticles are agglomerated in considerable amounts [22,23]. In addition to this Fig. 4b reveals that the TiO₂ nanoparticles successfully modified the surface of SMC resulting in the formation of the SMC-nTiO₂ adsorbent.

3.3. EDS analysis

Figs. 5a and b show the results of the energy-dispersive X-ray spectroscopy (EDS) of SMC and SMC-nTiO₂. From Table 1, the EDS analysis of SMC revealed the presence (at %) of O (56.54), Si (16.78), Al (6.04), Ti (0.30), Mg (2.01), Ca (14.45), Fe (3.65), and K (0.24). However, after modifying the composition changed to (at %) O (52.52), Si (10.53), Al (4.25), Ti (21.51), Mg (1.21), Ca (7.83), Fe (2.06), and K (0.09). The EDS confirmed the modifying of nano-TiO₂ onto the smectite.

3.4. BET surface area and pore characteristics

Specific surface areas of SMC and SMC-nTiO₂ particles were determined using BET analysis to be 28.121 and 46.255 $\text{m}^2 \text{g}^{-1}$, respectively. The increase in surface area is due to the coating of TiO₂ nanoparticles on the surface of the smectite [15].

3.5. Effect of SMC and SMC-nTiO₂ dosage

The effect of SMC and SMC-nTiO₂ dosage on the removal of RhB from their aqueous solutions is presented in Fig. 6. The removal percentage of RhB was studied at an initial concentration of 30 mg/L onto two adsorbents surfaces at 25°C. When the sorbent dosage was increased from 0.05 to 0.8 g, the removal of dye by SMC and SMC-nTiO₂ surfaces increased from 59% to 86% and from 92% to 99%, respectively. This may be simply attributed to the increase of SMC and SMC-nTiO₂ surface area and the availability of a greater number of sorption sites for the removal of RhB dye molecules [27]. Similar results were found by other authors [28,29].

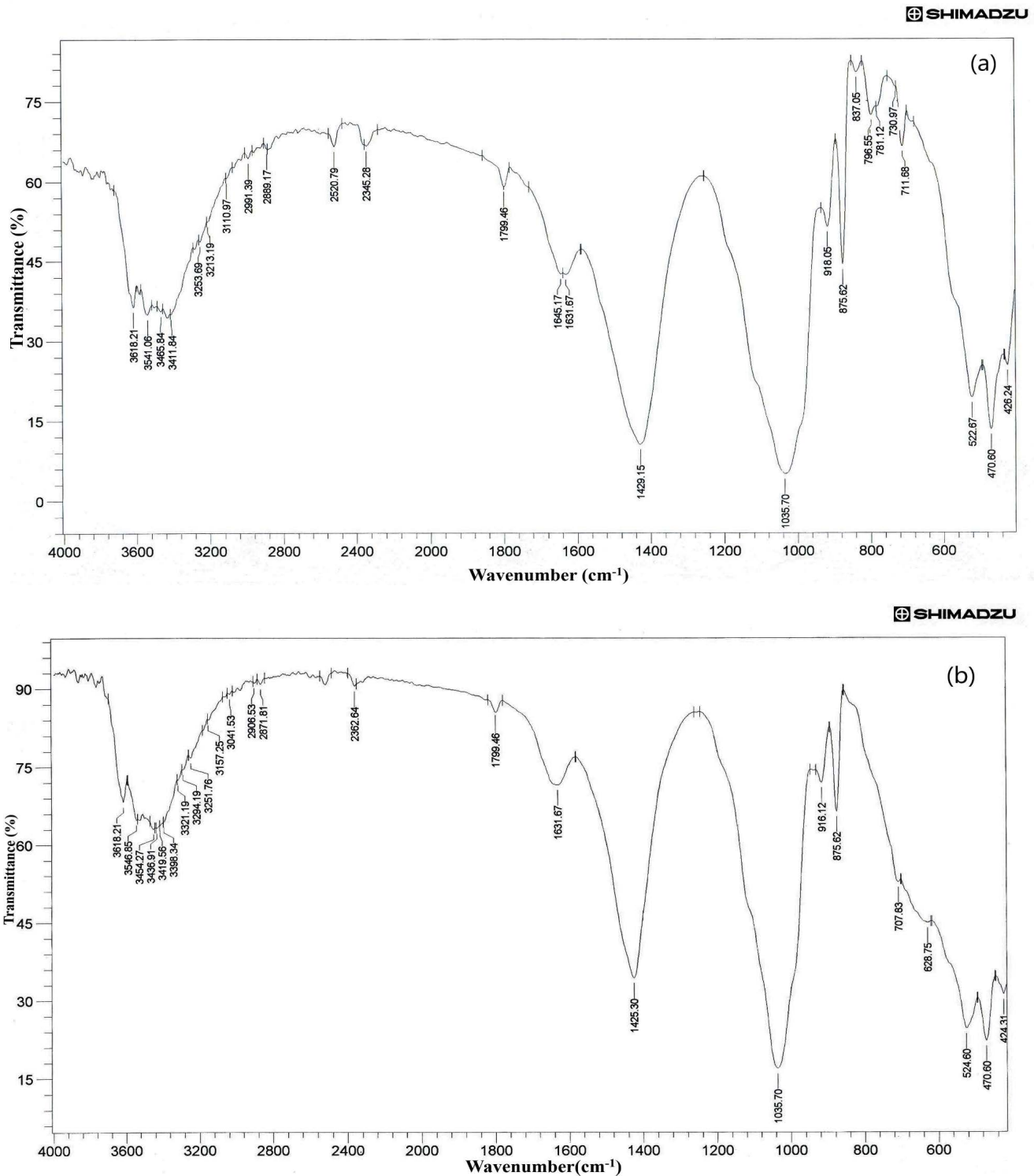


Fig. 3. FTIR spectra of: (a) SMC and (b) SMC-nTiO₂.

3.6. Effect of contact time

The effect of contact time on the removal of RhB onto SMC and SMC-nTiO₂ adsorbents was investigated at 30 mg/L, temperature 25°C, and pH 6.5. The results are presented in Fig. 7. The dye removal occurred rapidly

within a short period of time reaching equilibrium within 45 min for SMC and 35 min for SMC-nTiO₂, after which the adsorption became constant. There was also an evident significant increase in the amount of RhB adsorbed (q_e) for the two adsorbents studied due to greater availability of the active sorption sites and easier dye adsorption on

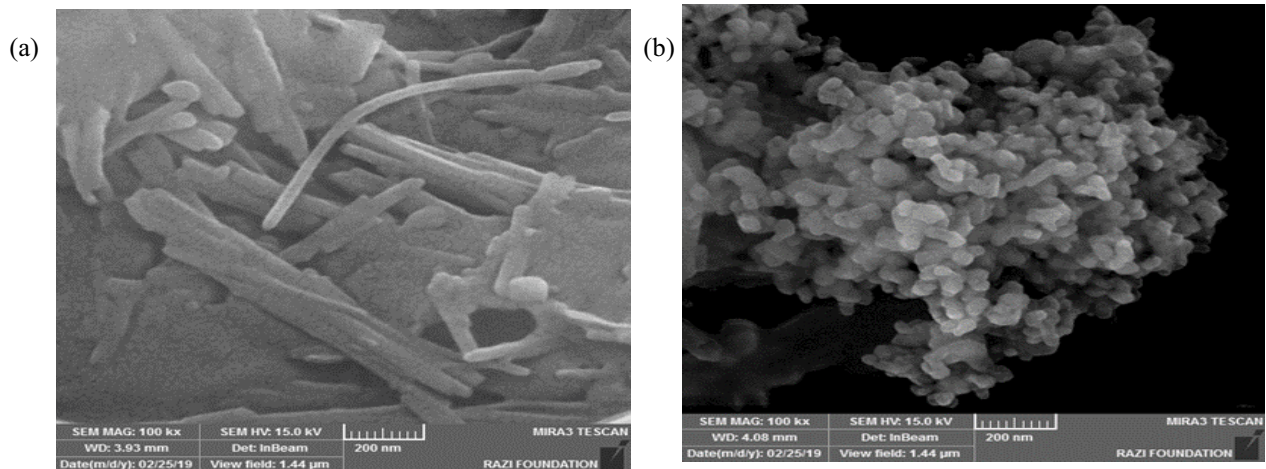


Fig. 4. SEM images of: (a) SMC surface and (b) SMC-nTiO₂ surface.

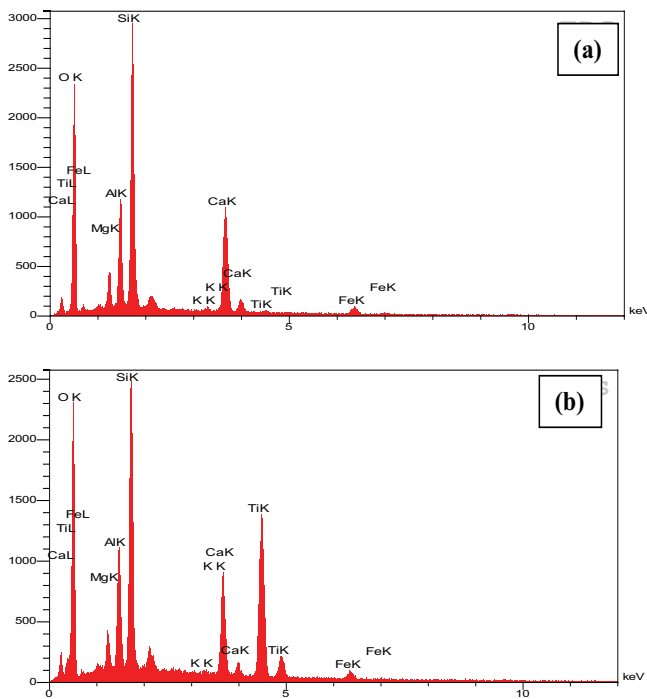


Fig. 5. EDS analysis of: (a) SMC and (b) SMC-nTiO₂.

the same sites, because the active sorption sites are more available and the dye ions are easily adsorbed on these sites. Similar observations have been made earlier [29,30].

3.7. Effect of pH solution on the RhB removal

The effect of pH on the RhB removal by SMC and SMC-nTiO₂ surfaces was studied at 25°C, initial dye concentration of 30 mg/L and adsorbent weight of 0.2 and 0.1 g, respectively. To obtain the required pH a few drops of 0.1 M HCl and NaOH were added. In Fig. 8a, the pH effect on the removal of cationic dye was presented. As the pH of the dye solution was increased, the R% increased from 60.0% to 91.4% and from 81.5% to 99.9% for SMC and

Table 1
Quantitative analysis results of EDS of SMC and SMC-nTiO₂

ELT	W _t % (SMC)	W _t % (SMC-nTiO ₂)
O	56.54	52.52
Mg	2.01	1.21
Al	6.04	4.25
Si	16.78	10.53
K	0.24	0.09
Ca	14.45	7.83
Ti	0.30	21.51
Fe	3.65	2.06

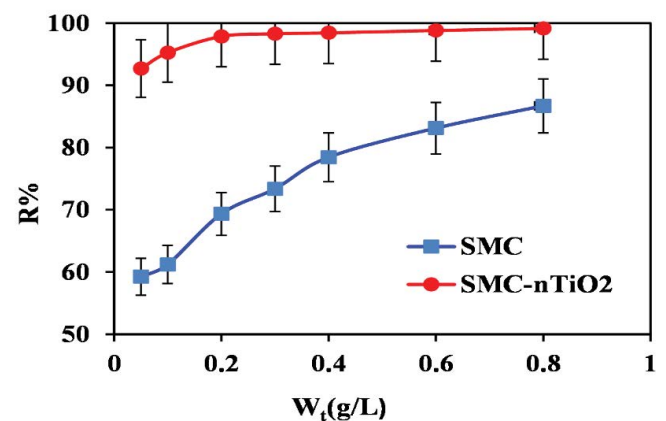


Fig. 6. Effect of adsorbent dosage on the removal of RhB onto SMC and SMC-nTiO₂ at 25°C and pH 6.5.

SMC-nTiO₂ surfaces, respectively. Lower adsorption of RhB at acidic pH is due to the presence of excess H⁺ ions competing with the positive species of dye for the active adsorption sites [31]. Moreover, the chief constituents of smectite are mainly Al and Si oxides. These metal oxides in aqueous solution tend to form metal-hydroxide complexes to yield a positively charged surface and dye molecules are highly in protonated form thus, electrostatic

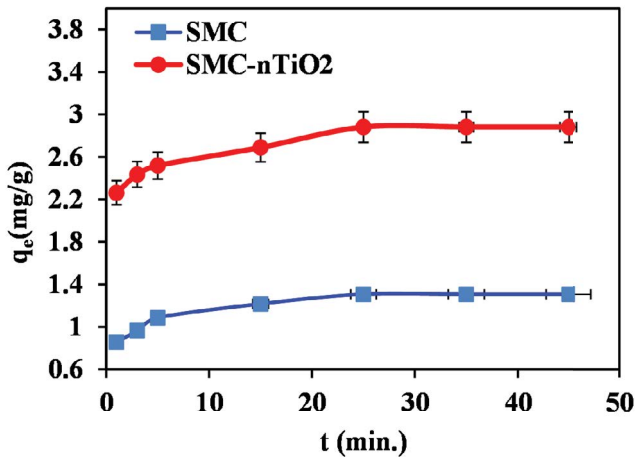


Fig. 7. Effect of contact time on the removal of RhB onto SMC and SMC-nTiO₂ at 25°C and pH 6.5.

repulsion between the positively charged RhB molecules and the positively charged surface leads to lower removal of dye [32]. The p*H*_{pzc} of the SMC and SMC-nTiO₂ was found to be 5.5 and 4.8, respectively, as presented in Fig. 8b, which further confirms the SMC and SMC-nTiO₂ surfaces can obtain positive charge at p*H* < p*H*_{pzc}. By contrast, the surfaces of SMC and SMC-nTiO₂ are negatively charged in basic medium, which causes the electrostatic attraction between the negatively charged surface and the dye cation. So, maximum removal of dye by smectite occurred at basic p*H*. Similar observation was reported by other investigators for the adsorption of basic dye [14,33].

3.8. Kinetic analysis

The kinetic data of RhB removal were tested using three types of mathematical models, pseudo-first-order (PFO) (Eq. (3)) [34], PSO (Eq. (4)) [35], and intra-particle diffusion models (Eq. (5)) [36]:

$$\ln(q_e - q_t) = \ln q_e - k_1 t \tag{3}$$

$$\frac{t}{q_e} = \frac{1}{k_2 q_e^2} + \frac{1}{q_e} t \tag{4}$$

$$q_t = k_{id} t^{0.5} + I \tag{5}$$

where *k*₁ (min⁻¹) and *k*₂ (g/mg min) are the rate constants [37], *q_e* and *q_t* (mg/g) are the amount of the RhB adsorbed at equilibrium and any contact time of adsorption *t* (min), respectively. The parameters (*q_e*, *k*₁, *k*₂, and *k*_{id}) in three models (first, second-order, and intra-particle diffusion) can be calculated experimentally from plotting ln(*q_e* - *q_t*) vs. *t* (Figs. 9a and b) and (*t/q_t*) vs. *t* (Figs. 10 a and b), respectively. *k*_{id}, the intra-particle diffusion rate constant (mg/g min^{0.5}) can be determined from the slope of the linear plot of *q_t* vs. *t*^{1/2} and *I* (mg/g) is a constant (Figs. 11a and b). Table 2 reveals that *R*² is better fitted to a PSO model than to the PFO and intra-particle diffusion models. Furthermore, the calculated (*q_e*) values (Table 2) are also closer to the unity of experimental (*q_e*) values for the PSO model than that for the PFO and intra-particle diffusion models at various temperatures. This indicates that the empirical second-order model can provide a more suitable description of the adsorption kinetics of RhB by SMC and SMC-nTiO₂ surfaces [15,38]. The low values of *R*² (Table 2) for the intra-particle diffusion model show that this model is not applicable [39]. Similar results were found by other authors [33,40]. The rate adsorption constant (*k*₂) can be explained as a function of temperature by the following Arrhenius equation:

$$\ln k_2 = \ln A - \frac{E_a}{RT} \tag{6}$$

where *E_a* is the activation energy (kJ mol⁻¹), *k*₂ is the PSO rate constant of dye removal, *A* is the Arrhenius factor, *R* is the gas constant (8.314 J K⁻¹ mol⁻¹), and *T* is the

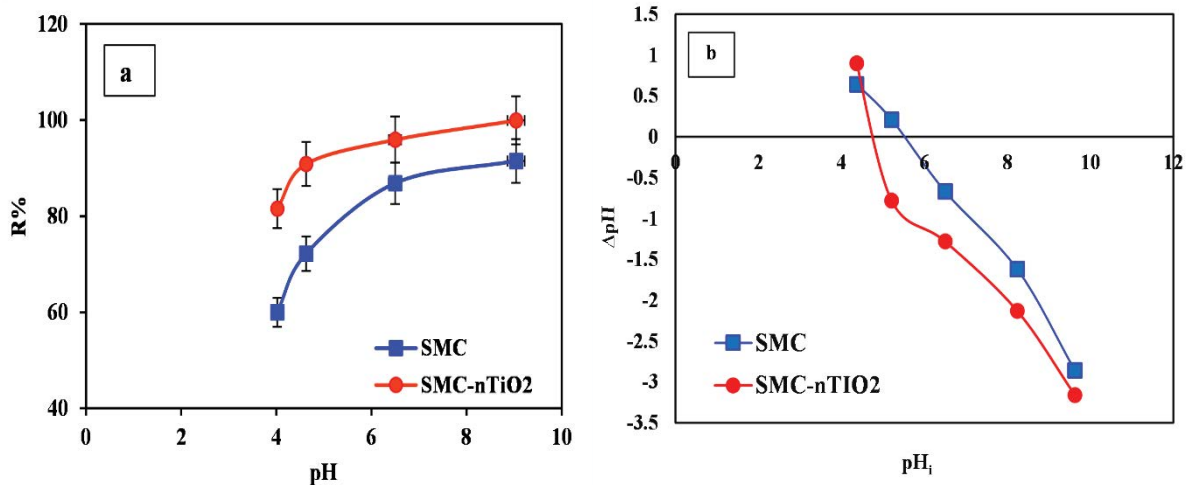


Fig. 8. (a) Effect of p*H* solution on the removal of RhB onto SMC and SMC-nTiO₂ surfaces and (b) p*H*_{pzc} of SMC and SMC-nTiO₂ surfaces at 25°C.

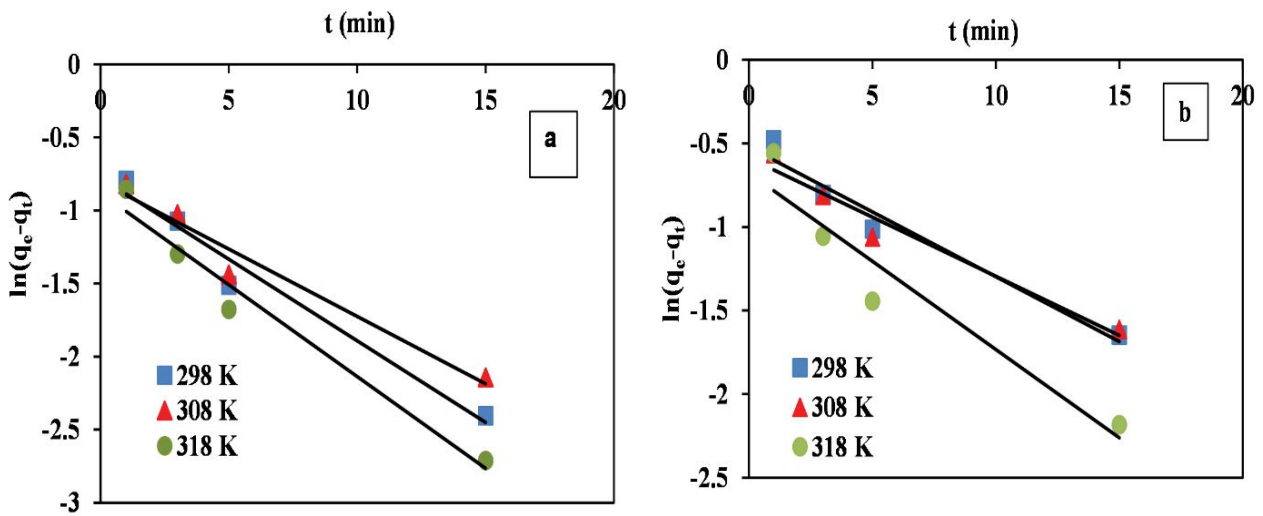


Fig. 9. Pseudo-first-order kinetics for RhB dye removal onto: (a) SMC and (b) SMC-nTiO₂ at different temperatures.

Table 2
Kinetics parameters for the removal of RhB onto SMC and SMC-nTiO₂ surfaces ($C_0 = 30$ mg/L)

Adsorbent	T (K)	Pseudo-first-order				Pseudo-second-order			Intra-particle diffusion		
		k_1 (min ⁻¹)	$q_{e,exp}$ (mg/g)	$q_{e,calc}$ (mg/g)	R^2	k_2 (g/mg min)	$q_{e,calc}$ (mg/g)	R^2	k_{id} (mg/g min ^{0.5})	I (mg/g)	R^2
SMC	298	0.1114	1.3070	0.4596	0.9706	2.7669	1.2722	0.9989	0.1242	0.7564	0.9471
	308	0.0920	1.3779	0.4472	0.9602	3.2312	1.3642	0.9982	0.1286	0.8157	0.9747
	318	0.1254	1.4507	0.4137	0.9703	5.3174	1.4326	0.9995	0.1188	0.9501	0.9215
SMC-nTiO ₂	298	0.0775	2.8813	0.5932	0.9596	62.8949	2.7472	0.9997	0.1418	2.1626	0.9521
	308	0.0707	2.9522	0.5556	0.9592	76.9242	2.8011	0.9997	0.1258	2.2842	0.9624
	318	0.1055	2.9992	0.5080	0.9164	92.0268	2.9411	0.9999	0.1492	2.3521	0.8677

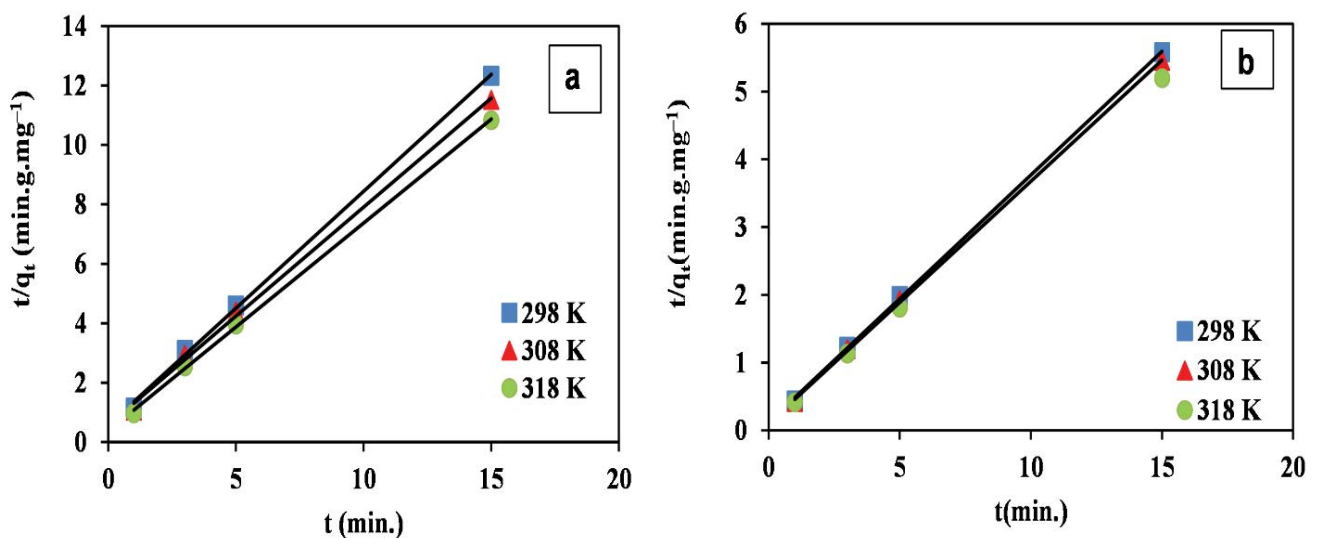


Fig. 10. Pseudo-second-order kinetics for RhB dye removal onto: (a) SMC and (b) SMC-nTiO₂ at different temperatures.

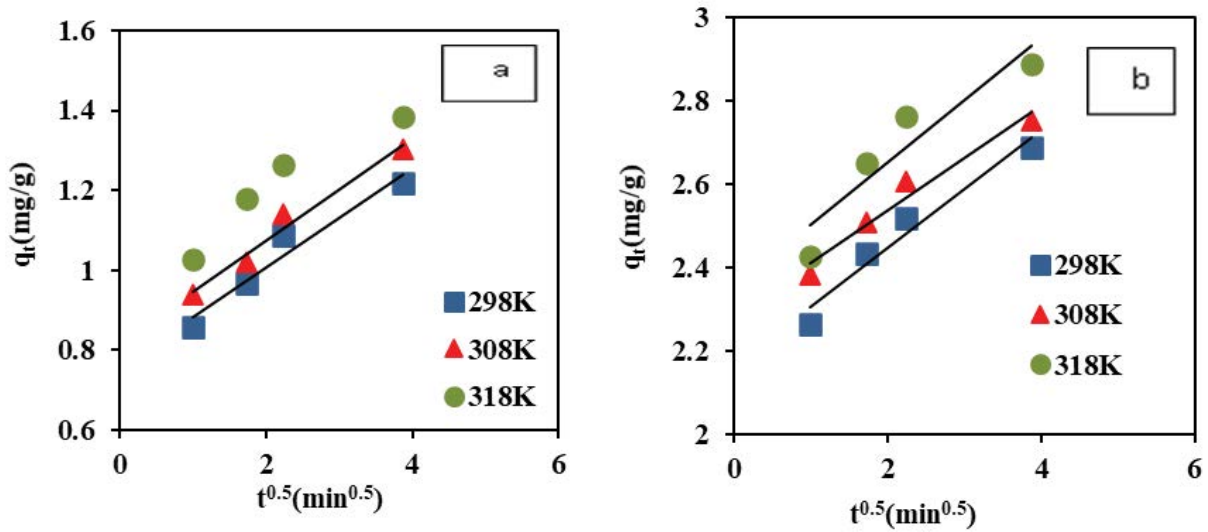


Fig. 11. Intra-particle diffusion for RhB dye removal onto: (a) SMC and (b) SMC-nTiO₂ at different temperatures.

temperature (Kelvin). A linear plot of $\ln k_2$ vs. $1/T$ (K^{-1}) for the RhB dye removal onto SMC and SMC-nTiO₂ is used to generate the value of E_a from the slope. The value of 25.57 and 14.99 kJ mol^{-1} for the activation energy of cationic dye onto SMC and SMC-nTiO₂ respectively, suggests that the removal mechanism is physisorption [41].

3.9. Equilibrium modeling

Figs. 12a and b show the adsorption isotherms of RhB at various temperatures. The adsorption capacity for RhB increases with the increasing equilibrium concentration of cationic dye. Higher temperature results in higher adsorption capacity.

Models of adsorption isotherms are used to describe the adsorption properties between the molecules of adsorbed dye and the adsorbent surface, the adsorbent capacity and to deduce the possibility of the adsorption process mechanism [42,43]. The Langmuir model

assumes that the homogenized adsorbent surface would be monolayer coverage of the adsorbate at a constant temperature [44]. The linearized Langmuir model is presented by the following equation:

$$\frac{C_e}{q_e} = \frac{1}{K_L q_m} + \frac{C_e}{q_e} \tag{7}$$

The Freundlich model, is typically used to describe the adsorption process on heterogeneous surfaces and is not limited to the formation of the monolayer [45]. The linearized form is expressed as:

$$\log q_e = \log K_f + \frac{1}{n} \log C_e \tag{8}$$

where q_m is the maximum amount of RhB dye adsorbed (mg/g), C_e is the equilibrium concentration of the cationic

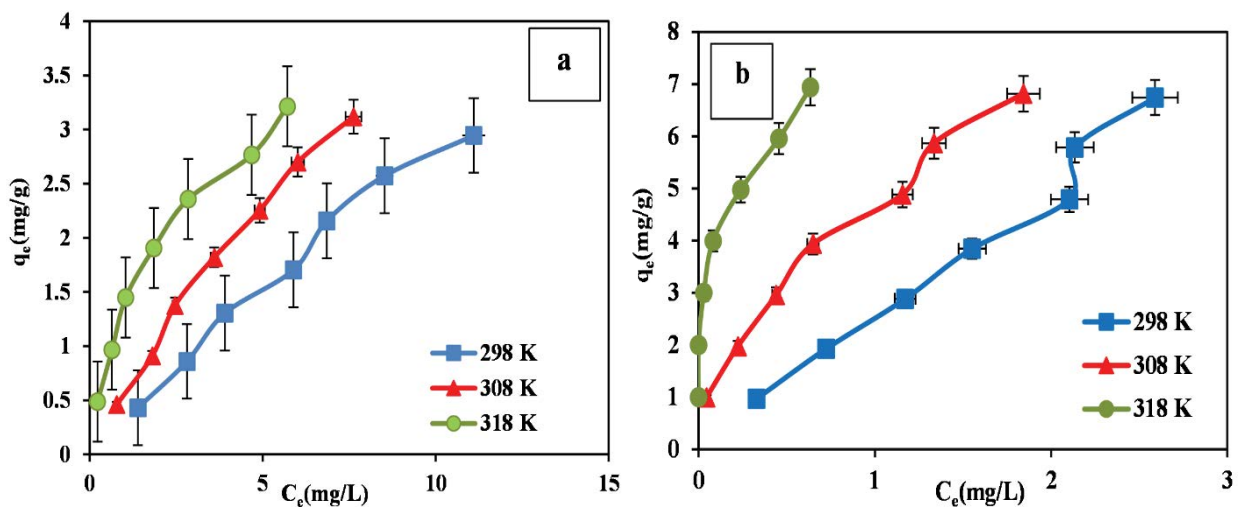


Fig. 12. Adsorption isotherms of RhB onto: (a) SMC and (b) SMC-nTiO₂ at different temperatures.

dye in solution (mg/g), K_L is Langmuir constant related to the adsorption energy (L/mg). q_m and K_L can be calculated from the slope and intercept of the plots of C_e/q_e vs. C_e . K_f and $1/n$ represent the Freundlich constants corresponding to the amount of dye adsorbed and the adsorption intensity, the magnitude of K_f and $1/n$ can be determined from the intercept and slope of the linear plot of $\log q_e$ vs. $\log C_e$.

The Temkin model suggests that the heat associated with the adsorption process of all molecules in the layer would decrease linearly with surface coverage because of the interactions between adsorbate and adsorbent [46]. The Temkin isotherm has been generally represented by the following equation:

$$q_e = B \ln A_T + B \ln C_e \quad (9)$$

where $B = RT/b$, b is the Temkin constant related to the heat of adsorption (J/mol), A is the Temkin isotherm constant (L/g), R is the gas constant (8.314 J/mol K), and T is the absolute temperature (K). The values of (B) and (A_T) can be determined from the slope and intercept, respectively, by the graph plotted between q_e and $\ln C_e$.

The detailed parameters of Langmuir, Freundlich, and Temkin model equations are reported in Table 3. The values of R^2 in Table 3, strongly indicate that the removal of basic dye (RhB) by SMC and SMC-TiO₂ follows the Freundlich isotherm model. Since the $1/n$ value is <1.0, it indicates favorable adsorption for natural SMC and nano-TiO₂ modified SMC [1,47] and high adsorption capacity [19]. Various adsorbent materials and their maximum adsorption capacities are listed in Table 4.

3.10. Thermodynamic investigation

Thermodynamic parameters including the change in standard free energy (ΔG°), standard enthalpy (ΔH°), and standard entropy (ΔS°) for the removal of RhB by SMC and SMC-nTiO₂ are estimated according to Eqs. (10) and (12) at three various temperatures – 298, 308, and 318 K [55]:

$$\Delta G^\circ = -RT \ln K^0 \quad (10)$$

where R is the gas constant (8.314 J/mol K) and T (Kelvin) is the temperature.

The distribution coefficient (K_d) can be expressed as:

$$K_d = \frac{C_0 - C_e}{C_e} \times \frac{V}{W} \quad (11)$$

where C_0 is the initial basic dye concentration and C_e is the equilibrium basic dye concentration in mg/L. V (mL) is the volume of the sample and W_i (g/L) is the weight of the adsorbent.

The change in standard enthalpy (ΔH°) and the change in standard entropy (ΔS°) were obtained using the following equation:

$$\ln K^0 = \frac{\Delta S^\circ}{R} - \frac{\Delta H^\circ}{RT} \quad (12)$$

The equilibrium constant (K^0) was estimated by plotting $\ln K_d$ against C_e and extrapolating C_e to 0. The value of the intercept is that of $\ln K^0$. The values of ΔH° and ΔS° were determined by plotting $\ln K^0$ vs. $1/T$ (K⁻¹) [32]. For (SMC and SMC-nTiO₂) systems, the negative magnitudes (–14.34, –16.35, and –19.80 kJ/mol), (–19.65, –24.20, and –29.55 kJ/mol), respectively, of standard free energy (ΔG°) at each temperature indicate the thermodynamic feasibility and spontaneity [56,57]. For two systems (SMC and SMC-nTiO₂) ΔH° positive magnitudes (66.68 and 127.81 kJ/mol) suggests that the removal of RhB is an endothermic process [58]. Moreover, endothermic nature is also reflected by the increase in the adsorbed amount of RhB with the raise of temperature [59]. Similarly the positive magnitudes of ΔS° indicate the increased randomness during the removal of dye by adsorption process so that increased entropy creates the replacement of hydrated ions of RhB dye for water molecules around adsorbent particles [60].

3.11. Data fitting

An error has been imposed to evaluate the fit of an isotherm model and the accuracy of the obtained experimental equilibrium data. In this research, the nonlinear Chi-square test was performed for Langmuir, Freundlich, and Temkin isotherm models. This can be represented mathematically as [61]:

Table 3
Isotherm parameters for RhB removal onto SMC and SMC-nTiO₂ surfaces

Isotherm	Adsorbent	298 K			308 K			318 K		
		K_L (L/mg)	q_m (mg/g)	R^2	K_L (L/mg)	q_m (mg/g)	R^2	K_L (L/mg)	q_m (mg/g)	R^2
Langmuir	SMC	1.6173	3.7453	0.9795	1.3700	2.5595	0.9848	0.5755	2.2212	0.9282
	SMC-nTiO ₂	0.0522	53.1914	0.2335	1.4671	8.6730	0.9147	30.0300	6.8027	0.9770
Freundlich	SMC	K_f	$1/n$	R^2	K_f	$1/n$	R^2	K_f	$1/n$	R^2
	SMC-nTiO ₂	0.3271	0.9490	0.9917	0.5804	0.8546	0.9935	1.2433	0.5746	0.9841
Temkin	SMC	2.6266	0.9278	0.9914	4.7632	0.5243	0.9914	7.5023	0.2612	0.9906
	SMC-nTiO ₂	B_T (J/mol)	A_T (L/g)	R^2	B_T (J/mol)	A_T (L/g)	R^2	B_T (J/mol)	A_T (L/g)	R^2
	SMC	1.2460	6.0699×10^{-3}	0.9499	1.1870	13.4960	0.9486	0.8430	1.7511	0.9720
	SMC-nTiO ₂	2.6662	2.2809	0.8836	1.5361	1.3617	0.8883	1.2097	1.1936	0.9623

Table 4
Comparison of maximum adsorption capacity of various adsorbents for the removal of RhB dye

Adsorbent	q_{\max} (mg/g)	References
Titania-silica	0.11	[48]
Zeolite MCM-22	1.11	[49]
Australian natural zeolite	2.12	[50]
Coal ash	2.86	[51]
<i>Magnifera indica</i> (Mango) leaf	3.00	[52]
Walnut shell	2.00	[53]
Synthesized hybrid ion exchanger	1.00	[54]
Natural bentonite	1.32	[16]
Purified bentonite	2.35	[16]
SMC	1.24	This study
SMC-nTiO ₂	7.50	

Table 5
Isotherm error analysis (χ^2) for removal of RhB onto SMC and SMC-nTiO₂ surfaces at different temperature

Adsorbent	Isotherm	298 K	308 K	318 K
SMC	Langmuir	22.3126	3.1170	2.3943
	Freundlich	3.0034	0.0279	1.6311
	Temkin	0.2739	0.3179	0.1606
SMC-nTiO ₂	Langmuir	0.1296	0.4216	3.4505
	Freundlich	0.1175	0.0752	0.0236
	Temkin	1.1293	1.2812	49.8088

$$\chi^2 = \sum_{i=1}^n \frac{(q_{\text{cal}} - q_{\text{exp}})^2}{q_{\text{exp}}} \quad (13)$$

where q_{cal} is the equilibrium amount of dye adsorbed obtained by calculating using the model (mg/g) and q_{exp} is the experimental data of the equilibrium amount of dye adsorbed (mg/g). The results of the application of non-linear Chi-square test (χ^2) are shown in Table 5. The Freundlich isotherm model appears to be the best fitting model for RhB removal onto SMC and SMC-nTiO₂ surfaces.

4. Conclusions

The sorbent SMC-nTiO₂ was successfully prepared by modifying titanium oxide nanoparticles onto Iraqi smectite clay and employed to remove RhB dye from aqueous solutions. The results indicate that SMC-nTiO₂ is a better adsorbent for the removal of cationic pollutants than SMC. Basic solution pH was proved to be more favorable for the removal of RhB on both adsorbent surfaces. RhB removal isotherm data were fitted well to the Freundlich isotherm model. The PSO kinetic model best explained the dynamic data for cationic dye removal on natural SMC and SMC-nTiO₂. Thermodynamic studies show that the RhB removal process was exothermic, spontaneous, favorable, and physisorption in nature. The experimental results

demonstrated that the SMC and SMC-nTiO₂ can be successfully used for the removal of basic dye from aqueous solutions.

Acknowledgments

The authors wish to thank for the support from the Chemistry Department, College of Education for pure science Ibn Al-Haitham, University of Baghdad.

References

- [1] K.G. Bhattacharyya, S. Sen Gupta, G.K. Sarma, Interactions of the dye Rhodamine B with kaolinite and montmorillonite in water, *Appl. Clay Sci.*, 99 (2014) 7–17.
- [2] K. Shen, M.A. Gondal, Removal of hazardous Rhodamine dye from water by adsorption onto exhausted coffee ground, *J. Saudi Chem. Soc.*, 21 (2017) S120–S127.
- [3] M.E. Mahmoud, G.M. Nabil, N.M. El-Mallah, S.B. Karar, Assessment of the adsorptive color removal of methylene blue dye from water by activated carbon sorbent-immobilized-sodium decyl sulfate surfactant, *Desal. Water Treat.*, 57 (2016) 8389–8405.
- [4] Z. Khan, O. Bashir, M.N. Khan, T.A. Khan, S.A. Al-Thabaiti, Cationic surfactant assisted morphology of Ag@Cu, and their catalytic reductive degradation of Rhodamine B, *J. Mol. Liq.*, 248 (2017) 1096–1108.
- [5] T.A. Khan, E.A. Khan, Adsorptive uptake of basic dyes from aqueous solution by novel brown linseed deoiled cake activated carbon: equilibrium isotherms and dynamics, *J. Environ. Chem. Eng.*, 4 (2016) 3084–3095.
- [6] Q. Wang, D. Gao, C. Gao, Q. Wei, Y. Cai, J. Xu, X. Liu, Y. Xu, Removal of a cationic dye by adsorption/photo degradation using electro spun PAN/O-MMT composite nanofibrous membranes coated with TiO₂, *Int. J. Photo Energy*, 2012 (2012) 1–8.
- [7] S. Song, A.L. Valdivieso, D.J.H. Campos, C. Peng, M.G.M. Fernandez, I. Razo-Soto, Arsenic removal from high-arsenic water by enhanced coagulation with ferric ions and coarse calcite, *Water Res.*, 40 (2006) 364–372.
- [8] F. Güzel, H. Saygılı, G.A. Saygılı, F. Koyuncu, New low-cost nanoporous carbonaceous adsorbent developed from carob (*Ceratonia siliqua*) processing industry waste for the adsorption of anionic textile dye: characterization, equilibrium and kinetic modeling, *J. Mol. Liq.*, 206 (2015) 244–255.
- [9] Q. Liu, B. Yang, L. Zhang, R. Huang, Adsorption of an anionic azo dye by cross-linked chitosan/bentonite composite, *Int. J. Biol. Macromol.*, 72 (2015) 1129–1135.
- [10] S. Noreen, H.N. Bhatti, S. Nausheen, S. Sadaf, M. Ashfaq, Batch and fixed bed adsorption study for the removal of Drimarine Black CL-B dye from aqueous solution using a lignocellulosic waste: a cost affective adsorbent, *Ind. Crops Prod.*, 50 (2013) 568–579.
- [11] J. Fu, Z. Chen, M. Wang, S. Liu, J. Zhang, J. Zhang, R. Han, Q. Xu, Adsorption of methylene blue by a high-efficiency adsorbent (polydopamine microspheres): kinetics, isotherm, thermodynamics and mechanism analysis, *Chem. Eng. J.*, 259 (2015) 53–61.
- [12] A. Shamsizadeh, M. Ghaedi, A. Ansari, A. Ansari, S. Zizian, M.K. Purkait, Tin oxide nanoparticle loaded on activated carbon as new adsorbent for efficient removal of malachite green-oxalate: non-linear kinetics and isotherm study, *J. Mol. Liq.*, 195 (2014) 212–218.
- [13] V. Gupta, D. Mohan, S. Sharma, M. Sharma, Removal of basic dyes (Rhodamine B and Methylene Blue) from aqueous solutions using bagasse fly ash, *Sep. Sci. Technol.*, 35 (2000) 2097–2113.
- [14] T.A. Khan, S. Dahiya, I. Ali, Use of kaolinite as adsorbent: equilibrium, dynamics and thermodynamic studies on the adsorption of Rhodamine B from aqueous solution, *Appl. Clay Sci.*, 69 (2012) 58–66.

- [15] Y. Yu, B.N. Murthy, J.G. Shapter, K.T. Constantopoulou, N.H. Voelcker, A.V. Ellis, Benzene carboxylic acid derivatized graphene oxide nanosheets on natural zeolites as effective adsorbents for cationic dye removal, *Kristina T. Constantopoulou, Nicolas H. Voelcker, Amanda V. Ellis, J. Hazard. Mater.*, 260 (2013) 330–338.
- [16] J.F.D. Neto, I.D.S. Pereira, V.C. da Silva, H.C. Ferreira, G.A. Neves, R.R. Menezes, Study of equilibrium and kinetic adsorption of rhodamine B onto purified bentonite clays, *Cerâmica*, 64 (2018) 598–607.
- [17] R.F. Giese, C.J. Van Oss, M. Dekker, *Colloid And Surface Properties of Clays and Related Minerals*, CRC Press, New York NY, 2002.
- [18] P. Mpofo, J.A. Mensah, J. Ralston, Interfacial chemistry, particle interactions and improved dewatering behaviour of smectite clay dispersions, *Int. J. Miner. Process.*, 75 (2005) 155–171.
- [19] H. Sadegh, G.A.M. Ali, Z. Abbasi, M.N. Nadagouda, Adsorption of ammonium ions onto multi-walled carbon nanotubes, *Stud. UBB Chem.*, 62 (2017) 233–245.
- [20] W. Xu, Y. Chen, W. Zhang, B. Li, Fabrication of graphene oxide/bentonite composites with excellent adsorption performances for toluidine blue removal from aqueous solution, *Adv. Powder Technol.*, 30 (2019) 493–501.
- [21] J. Yin, C. Deng, Z. Yu, X. Wang, G. Xu, Effective removal of lead ions from aqueous solution using nano illite/smectite clay: isotherm, kinetic, and thermodynamic modeling of adsorption, *Water*, 10 (2018) 1–13.
- [22] M. Ramazani, M. Farahmandjou, T.P. Firoozabadi, Effect of nitric acid on particle morphology of the nano-TiO₂, *Int. J. Nanosci. Nanotechnol.*, 11 (2015) 115–122.
- [23] L. Chunxiang, G. Jie, P. Jianming, Z. Zulei, Y. Yongsheng, Synthesis, characterization, and adsorption performance of Pb(II)-imprinted polymer in nano-TiO₂ matrix, *J. Environ. Sci.*, 21 (2009) 1722–1729.
- [24] W. Zhang, Y. Wu, J. Wang, J. Liu, H. Lu, S. Zhai, Q. Zhong, S. Liu, W. Zhong, C. Huang, X. Yu, W. Zhang, Y. Chen, Adsorption of thallium(I) on rutile nano titanium dioxide and environmental Implications, *Peer J.*, 7 (2019) 1–16.
- [25] S. Bhattacharya, Studies on preparation and analysis of organoclay nano particles, *J. Eng. Sci.*, 3 (2014) 10–16.
- [26] S. Liu, Y. Ding, P. Li, K. Diao, X. Tan, F. Lei, Y. Zhan, Q. Li, B. Huang, Z. Huang, Adsorption of the anionic dye Congo red from aqueous solution onto natural zeolites modified with N,N-dimethyl dehydroabietylamine oxide, *Chem. Eng. J.*, 248 (2014) 135–144.
- [27] J.N. Ganguli, S. Agarwal, Removal of a basic dye from aqueous solution by a natural kaolinitic clay - adsorption and kinetic studies, *Adsorpt. Sci. Technol.*, 30 (2012) 171–182.
- [28] S. Chang, K. Wang, H. Li, M. Wey, J. Chou, Enhancement of Rhodamine B removal by low-cost fly ash sorption with Fenton pre-oxidation, *J. Hazard. Mater.*, 172 (2009) 1131–1136.
- [29] V. Kumar, Adsorption kinetics and isotherms for the removal of rhodamine B dye and Pb²⁺ ions from aqueous solutions by a hybrid ion-exchanger, *Arabian J. Chem.*, 12 (2019) 316–329.
- [30] L. Leng, X. Yuan, G. Zeng, J. Shao, X. Chen, Z. Wu, H. Wang, X. Peng, Surface characterization of rice husk bio-char produced by liquefaction and application for cationic dye (Malachite green) adsorption, *Fuel*, 155 (2015) 77–85.
- [31] D.E. Al-Mammar, Decolorization of the aqueous Safranin O dye solution using *Thuja orientalis* as biosorbent, *Iraqi J. Sci.*, 55 (2014) 886–898.
- [32] K. Kadirvelu, C. Karthika, N. Vennilamani, S. Patabhi, Activated carbon from industrial solid waste as an adsorbent for the removal of Rhodamine-B from aqueous solution: kinetic and equilibrium studies, *Chemosphere*, 60 (2005) 1009–1017.
- [33] M. Wang, J. Fu, Y. Zhang, Z. Chen, M. Wang, J. Zhu, W. Cui, J. Zhang, Q. Xu, Removal of Rhodamine B, a cationic dye from aqueous solution using poly(cyclotriphosphazene-co-4,40-sulfonyldiphenol) nanotubes, *J. Macromol. Sci. Part A Pure Appl. Chem.*, 52 (2015) 105–113.
- [34] S. Lagergren, About the theory of so-called adsorption of soluble substances, *Kungl. Svens. Vetenskapskad. Handl.*, 24 (1898) 1–39.
- [35] Y.S. Ho, G. McKay, Comparative sorption kinetic studies of dyes and aromatic compounds onto fly ash, *J. Environ. Sci. Health., Part A*, 34 (1999) 1179–1204.
- [36] M.A. Ahmad, R. Alrozi, Removal of malachite green dye from aqueous solution using rambutan peel-based activated carbon: equilibrium, kinetic and thermodynamic studies, *Chem. Eng. J.*, 171 (2011) 510–516.
- [37] M.R. Al-Kazragi, D.T.A. Al-Heetimi, O.S.A. Al-Khazrajy, Xylenol orange removal from aqueous solution by natural bauxite (BXT) and BXT-HDTMA: kinetic, thermodynamic and isotherm modeling, *Desal. Water Treat.*, 145 (2019) 369–377.
- [38] P. Panneer Selvam, S. Preethi, P. Basakaralingam, N. Thinakaran, A. Sivasamy, S. Ivanesan, Removal of Rhodamine B from aqueous solution by adsorption onto sodium montmorillonite, *J. Hazard. Mater.*, 155 (2008) 39–44.
- [39] M. Ghaedi, M. Pakniat, Z. Mahmoudi, S. Hajati, R. Sahraei, A. Daneshfar, Synthesis of nickel sulfide nanoparticles loaded on activated carbon as a novel adsorbent for the competitive removal of Methylene blue and Safranin-O, *Spectrochim. Acta, Part A*, 123 (2014) 402–409.
- [40] Z. Qi, Q. Liu, Z. Zhu, Q. Kong, Q. Chen, Ch. Zhao, Y. Liu, M. Miao, C. Wang, Rhodamine B removal from aqueous solutions using loofah sponge and activated carbon prepared from loofah sponge, *Desal. Water Treat.*, 57 (2016) 29421–29433.
- [41] L. Cottet, C.A.P. Almeida, N. Naidek, M.F. Viante, M.C. Lopes, N.A. Debacher, Adsorption characteristics of montmorillonite clay modified with iron oxide with respect to methylene blue in aqueous media, *Appl. Clay Sci.*, 95 (2014) 25–31.
- [42] X. Jin, B. Yu, Z. Chen, J.M. Arocena, R.W. Thring, Adsorption of Orange II dye in aqueous solution onto surfactant-coated zeolite: characterization, kinetic and thermodynamic studies, *J. Colloid Interface Sci.*, 435 (2014) 15–20.
- [43] T. Wang, P. Zhao, N. Lu, H. Chen, C. Zhang, X. Hou, Facile fabrication of Fe₃O₄/MIL-101(Cr) for effective removal of acid red 1 and orange G from aqueous solution, *Chem. Eng. J.*, 295 (2016) 403–413.
- [44] I. Langmuir, The adsorption of gases on plane surfaces of glass, mica and platinum, *J. Am. Chem. Soc.*, 40 (1918) 1361–1403.
- [45] H.M.F. Freundlich, Over the adsorption in solution, *J. Phys. Chem.*, 57 (1906) 1100–1107.
- [46] H. Zheng, D. Liua, Y. Zheng, S. Liang, Z. Liu, *J. Hazard. Mater.*, 167 (2009) 141–147.
- [47] S.A. Ali, I.B. Rachman, T.A. Saleh, Simultaneous trapping of Cr(III) and organic dyes by a pH-responsive resin containing zwitterionic aminomethyl phosphonate ligands and hydrophobic pendants, *Chem. Eng. J.*, 330 (2017) 663–674.
- [48] P.V. Messina, P. Schulz, Adsorption of reactive dyes on titanica-silica mesoporous materials, *J. Colloid Interface Sci.*, 299 (2006) 305–320.
- [49] S. Wang, H. Li, L. Xu, Application of zeolite MCM-22 for basic dye removal from waste water, *J. Colloid Interface Sci.*, 295 (2006) 71–78.
- [50] S. Wang, Z.H. Zhu, Characterization and environmental application of an Australian natural zeolite for basic dye removal from solution, *J. Hazard. Mater.*, 136 (2006) 946–952.
- [51] S. Wang, M. Soudi, L. Li, Coal ash conversion into effective adsorbent for removal of heavy metals and dyes from waste water, *J. Hazard. Mater.*, 133 (2006) 243–251.
- [52] S. Sharma, A. Imran, Adsorption of Rhodamine B dye from aqueous solution onto acid activated mango (*Mangifera indica*) leaf powder: equilibrium, kinetic and thermodynamic studies, *J. Toxicol. Environ. Health Sci.*, 3 (2011) 286–297.
- [53] J. Shah, M.R. Jan, A. Haq, Y. Khan, Removal of Rhodamine B from aqueous solutions and wastewater by walnut shells: kinetics, equilibrium and thermodynamics studies, *Front. Chem. Sci. Eng.*, 7 (2013) 428–436.
- [54] V. Kumar, B.S. Kaith, R. Jindal, Synthesis of hybrid ion exchanger for rhodamine B dye removal: equilibrium, kinetic and thermodynamic studies, *Ind. Eng. Chem. Res.*, 55 (2016) 10492–10499.
- [55] M. Constantin, I. Asmarandei, V. Harabagiu, L. Ghimici, P. Ascenzi, G. Fundueanu, Removal of anionic dyes from

- aqueous solutions by an ion-exchanger based on pullulan microspheres, *Carbohydr. Polym.*, 91 (2013) 74–84.
- [56] S. Muzaffar, H. Tahir, Enhanced synthesis of silver nanoparticles by combination of plants extract and starch for the removal of cationic dye from simulated waste water using response surface methodology, *J. Mol. Liq.*, 252 (2018) 368–382.
- [57] D.T.A. Heetimi, A.H. Dawood, Q.Z. Khalaf, T.A. Himdan, Removal of methyl orange from aqueous solution by Iraqi bentonite adsorbent, *Ibn Al-Haitham J. Pure Appl. Sci.*, 25 (2012) 1–13.
- [58] A. Maicaneanu, J.B.B. Mbah, C.C. Ndjeumi, L.C. Cotet, R.D. kanga, Physico-chemical properties and crystal violet adsorption performances of H_3PO_4 -modified mango seeds kernel, *Stud. UBB Chem.*, 63 (2016) 195–214.
- [59] Y. Miyah, A. Lahrichi, M. Idrissi, S. Boujraf, H. Taoudaand, F. Zerrouq, Assessment of adsorption kinetics for removal potential of Crystal Violet dye from aqueous solutions using Moroccan pyrophyllite, *J. Assoc. Arab Univ. Basic Appl. Sci.*, 23 (2017) 20–28.
- [60] U.J. Etim, S.A. Umoren, U.M. Eduok, Coconut coir dust as a low-cost adsorbent for the removal of cationic dye from aqueous solution, *J. Saudi Chem. Soc.*, 20 (2016) S67–S76.
- [61] K.Y. Foo, B.H. Hameed, Insights into the modeling of adsorption isotherm systems, *Chem. Eng. J.*, 156 (2010) 2–10.